DEVELOPMENT OF C-BAND ACCELERATING SECTION FOR SUPERKEKB

T. Kamitani*, N. Delerue, M. Ikeda, K. Kakihara, S. Ohsawa, T. Oogoe, T. Sugimura,
T. Takatomi, S. Yamaguchi, K. Yokoyama, KEK, Tsukuba, Japan
Y. Hozumi, Graduate University for Advanced Studies Department
of Accelerator Science, Tsukuba, Japan

Abstract

In a future luminosity upgrade from the present KEK-B factory to the SuperKEKB, the injector linac is required to increase the positron acceleration energy from 3.5 GeV to 8.0 GeV. It could be realized by replacing some of the present S-band accelerator modules to the C-band module and doubling the acceleration field gradient (21 → 42 MV/m). Research and development of the components for the C-band module has been performed since 2002. This paper reports on the development of the first prototype of the C-band accelerating section whose design is based on a half-scale dimension of the present S-band 2-m long section. Details in the design and the fabrication are described. Results of the high-power test, beam acceleration test and ten months' operation in the KEKB injector linac are given.

INTRODUCTION

The KEK-B factory has achieved the world highest luminosity of 1.39×10^{34} cm^{-2}s^{-1} [1] but further upgrade aiming 2.5×10^{35} cm^{-2}s^{-1} has been considered [2]. In this upgrade, the stored beam energies of the electrons (8.0 GeV) and of the positrons (3.5 GeV) will be exchanged against positron beam-instability due to the electron-cloud effect. Consequently, the injector linac has to increase positron acceleration energy from 3.5 GeV to 8.0 GeV. In the present injector, the positron generation target is placed in the midway of the linac. Only the accelerator modules after the target contributes to the positron acceleration and it is sufficient for 3.5-GeV injection but not for 8.0 GeV. The 8.0-GeV positron beam is obtained if we could double the acceleration field gradient (21 → 42 MV/m). It is a general strategy to use higher rf frequency for higher field gradient as seen in the active R and D works for the linear colliders [3]. We have adopted the C-band (5712 MHz) accelerator module to replace some of the present S-band (2856 MHz) modules. The rf frequency is exactly twice of the present S-band frequency to accomodate the remaining S-band modules. Design studies of the C-band components have been performed to fit them to the specification for the KEKB injector upgrade [4]. The C-band accelerating section which cope with the rf breakdowns in the structure is one of the key components in the C-band accelerator module development.

* takuya.kamitani@kek.jp

DESIGN AND FABRICATION

The design of the first prototype of the C-band accelerating section is based on a half-scale dimension of the present 2 m long S-band section used in the KEKB linac [5]. We could take advandages of determining many design parameters just by scaling. Thus, the length of the first prototype C-band section is 1 m. It has a disk-loaded waveguide structure whose disk-iris diameter decrease linearly along the section to achieve quasi-constant field gradient. Specifications and a figure of the C-band section are shown in Table 1 and in Fig. 1.

Table 1: Specifications of the first prototype 1-m long C-band accelerating section.

operation frequency	5712.000 (MHz)
operation temperature	30.0 (degC)
no. of cells	54 regular cells + 2 couplers
section length	926.225 (mm) (55 cells)
phase advance per cell	$\frac{2\pi}{3}$-mode
cell length	17.495 (mm)
disk thickness (t)	2.500 (mm)
iris diameter (2a)	12.475 ∼ 10.450 (mm)
cavity diameter (2b)	41.494 ∼ 41.010 (mm)
shunt impedance (r_0)	74.6 ∼ 85.1 (MΩ/m)
Q factor	9703 ∼ 9676 (mm)
group velocity (v_g/c)	1.9 ∼ 1.0 (%)
filling time	234 (ns)
attenuation parameter (τ)	0.434

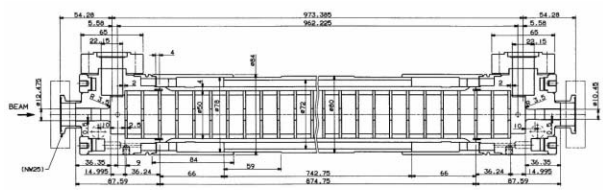

Figure 1: First prototype of C-band accelerating section.

The disks and cylindrical spacers forming regular cells of the accelerating section were made of oxygen-free copper and individually machined. The inner diameters of the spacers were adjusted by the Nodal shift measurements to achieve $2\pi/3$ phase advance per cell. After this resonant frequency adjustment of each cell, the central 50 cells out of total 54 cells were joined together by electroplating with copper. Typical radial thickness of the spacers was 4 mm

and the thickness of the electroplated copper layer outside the spacers was also 4 mm. After the electroplating process, an average resonant frequency was increased by 660 kHz, which is almost twice larger than an expectation from the S-band cases. It is supposed to come from the mismanagement of the solution concentration used in the electroplating. Besides this global frequency shift, the effect was locally smaller in the cells at both ends. It is due to the thinner electroplated layer for interface. The phase advances in these cells are 3 - 8 degrees less than the ordinary $2\pi/3$. Special care should be taken for these cells in the fabrication of the second prototype.

The couplers of the C-band section are single-feed type which magnetically couples the cavity to the waveguide through a thin small iris. While the dimensions of the regular cells could be half-scale of that of the S-band section, the coupler cells were not the case because the C-band waveguide (WR-187) connected to the coupler was not the half-scale of the S-band waveguide (WR-284). Original S-band coupler has dip structure at the opposite side from the coupling iris in order to compensate the field asymmetry. However, the high power study with the S-band structure has shown that the dip caused rf breakdowns. Thus, the dip was omitted in the first prototype C-band section and the field asymmetry was neglected. Optimum dimensions of the coupler cavity diameter and the coupling iris were approximately estimated with MAFIA-T3 simulation and precisely determined using low-power models by an iteration of the rf measurement (Kyhl method) and the machining of the cavity. Fabricated coupler cavities were jointed by the electron-beam welding (EBW) with the regular cells which were already united. Subsequently, a stainless-steel jacket for a cooling water layer was attached outside the structure by the tungsten inert gas (TIG) welding. After the EBW and TIG welding, the average resonant frequency went down by 300 kHz probably due to a deformation. Fortunately, this effect almost compensated for the excessive frequency shift by the electroplating, which resulted in the frequency deviation less than 100 kHz.

HIGH-POWER TEST

A test stand was built beside the KEKB linac for rf processing and high-power tests of the C-band components. After the high power tests of the klystron, the modulator, the sub-booster klystron, the rf window, the 3-db coupler and the dummy loads, the C-band accelerating section has installed in the test stand. rf pulse from the klystron in 500 ns duration was fed to the accelerating section at 50 Hz pulse repetition. After total 300 hours of rf processing (54 million rf pulse shots), it reaches to the level of 43.7-MW klystron output power which corresponds to the acceleration field of 41.8 MV/m assuming a theoretical shut impedance, as shown in Fig. 2.

Even at the end of the rf processing, rf breakdowns occur frequently, about ten times an hour at the highest power level. To investigate the breakdown location, rf pulse

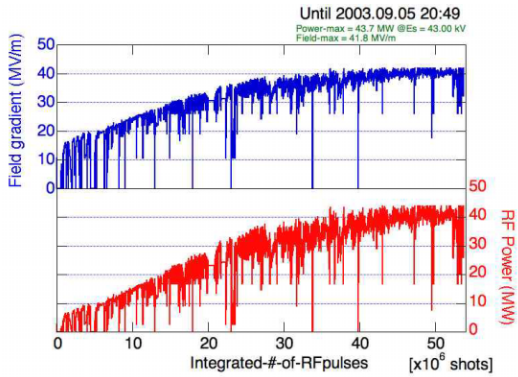

Figure 2: rf processing history.

shapes of incoming, outgoing and reflected waves of the accelerating structure were observed at each breakdown and numerically analyzed [6]. It is assumed that at the instant of rf breakdown the accelerating structure is locally short-circuited. The rf pulse propagating in the structure is divided there. Front part of the pulse propagetes forward and is observed as a terminated outgoing wave. Rear part of the pulse is reflected at the breakdown point, propagetes backward and is observed as a reflected wave. From the pulse length of the terminated outgoing wave, we can know that in what timing of the rf pulse the breakdown occurs. Figure 3(a) shows a distribution of the breakdown timing in an rf pulse. The distribution is rather flat except a peak at the beginning of the rf pulse. Likewise, information of the breakdown location can be obtained from the time difference between the end of the outgoing wave and the arrival of the reflected wave, as seen in Fig. 3(b). In this plot, the right-hand side is the input coupler and the left-hand side is the output coupler. We can see that the breakdown locations are concentrated around the input coupler.

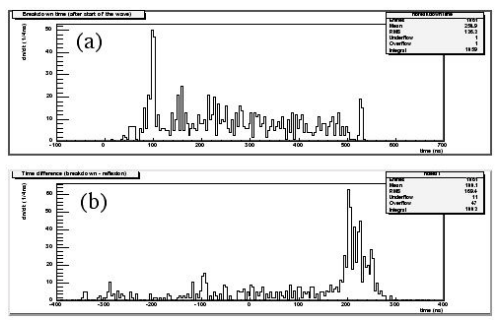

Figure 3: Breakdown location from rf pulse timing.

Acoustic sensors were also used to estimate the breakdown locations by detecting vibrations due to the breakdown [6]. Four sensors were attached on the input coupler, on the output coupler and at 1/3 and at 2/3 positions of the accelerating section in equal interval. The timing and the magnitude of the signals from the sensors were analyzed. Figure 4(a) shows a correlation between the fastest signal sensor and the largest signal sensor and figure 4(b) shows a distribution of which sensor had the fastest and the largest signal. It also suggest that most of the breakdowns occur around the input coupler.

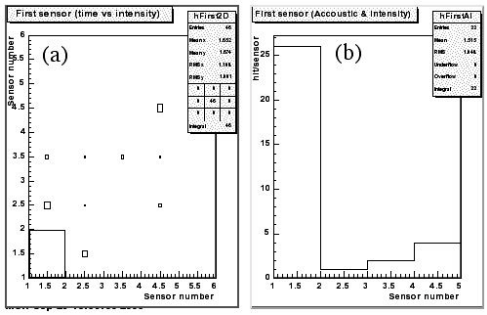

Figure 4: Breakdown location from acoustic sensor.

BEAM ACCELERATION TEST

In September of 2003, after finishing the rf processing and the high power test of the accelerating section at the test stand, a C-band accelerator module was constructed in the area of the S-band module No. 4-4 of the KEKB injector linac, which was temporary empty. A C-band klystron, the accelerating section and an rf dummy load were moved there from the test stand. A modulator and a low-power rf source including sub-booster klystron were newly installed. Unlikely to the design of a complete C-band accelerator module, only single 1-m long accelerating section was installed instead of two 2-m long sections and an rf pulse compressor was missing because it was still in a design stage. Recent status of the development of the pulse compressor will be reported by another paper in this conference [7]. In the operation of the C-band accelerator module, its energy gain has been measured at the energy analyzer in the end of the linac by changing the acceleration phase. We have used 3.0-GeV electron beams of 0.13-nC charge per pulse for injecting into the AR-SOR ring because of sufficiently good energy resolution and small beam-loading effect. Figure 5 shows that the energy gain was estimated to be 39.7 MeV which corresponds to the acceleration field of 41.2 MV/m with the klystron output power of 43.8 MW. The errors in individual data points comes from the measurement error of the beam positions. Besides these errors, the beam orbit displacement due to the field asymmetry in the couplers affects the result. This systematic error is supposed to be more than five percent, but yet to be studied.

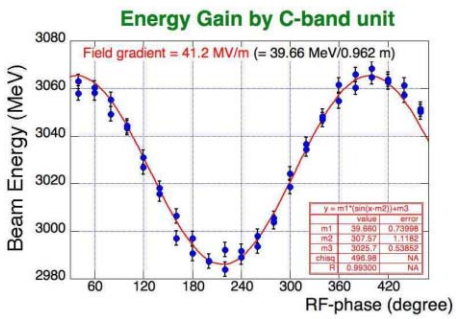

Figure 5: Measured energy gain of the C-band module.

LONG TERM OPERATION

The C-band module has been used for beam acceleration for ten months. The rf breakdown rate has become lower than the beginning, but is still five times an hour above 40 MW power level. After the ten months' operation, we have observed inside of the accelerating section using a CCD endoscope. As seen in Fig. 6(a), the iris edge in the input coupler were discolored and the surface in the suburb of the iris was turned into black. In the output coupler, these damages were not so obvious. Damage of the disk iris with plenty of small pits can be seen in Fig. 6(b). It was remarkable in the first disk connecting to the input coupler cell, but much less in the second and third disks and further less in the disks close to the output coupler. These locations of the surface damage are consistent with the distribution of the breakdown locations. In the second prototype accelerating section, we adopt thicker coupling iris, and tuning of the coupler dimension using low-power models is in progress.

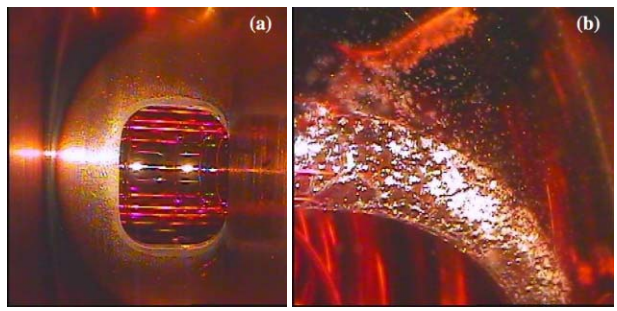

Figure 6: Surface damage in accelerating structure.

ACKNOWLEDGEMENT

The authors wish to thank Mitsubishi Heavy Industries, Ltd. and Mechanical Engineering Center of KEK for their cooperation in fabricating the accelerating section.

REFERENCES

[1] KEKB, An Asymmetric Electron-Positron Collider for B Physics, http://www-acc.kek.jp/KEKB/.

[2] SuperKEKB Letter of Intent (LoI), KEK Report 04-4, August, 2004, http://belle.kek.jp/superb/loi/.

[3] X-band R and D for GLC, http://lcdev.kek.jp/
C-band R and D for GLC and X-ray FEL,
http://c-band.kek.jp/.

[4] T. Kamitani, et. al., "R and D status of C-band accelerating unit for SuperKEKB", PAC2003 conference, Portland, OR, USA, 12-16 May 2003.

[5] I. Abe, et. al., "The KEKB injector linac", KEK Preprint 2001-157, Nucl. Instrum. Methods A, Volume 499, Issue 1, 21 February 2003, Pages 167-190.

[6] N. Delerue, "Identifying high power breakdowns in accelerating structures with acoustic sensors",
http://acfahep.kek.jp/appi/2004/TPs/Nicolas0402appi.pdf.

[7] T. Sugimura et. al., "SKIP - A pulse compressor for SuperKEKB", This proceedings.